Optical Materials 31 (2009) 1853–1856

Contents lists available at ScienceDirect

Optical Materials

journal homepage: www.elsevier.com/locate/optmat

ZnO sputter coating on SnO_2 nanowires: Effects of thin coating and subsequent thermal annealing

Hyoun Woo Kim *, Mesfin Abayneh Kebede, Hyo Sung Kim

Division of Materials Science and Engineering, Inha University, Incheon 402-751, Republic of Korea

ARTICLE INFO

Article history:
Received 13 July 2008
Received in revised form 8 September 2008
Accepted 10 December 2008
Available online 5 May 2009

PACS:
81.07.−b
81.05.Dz
78.55.−m
61.10.Nz
68.37.Lp

Keywords:
SnO_2
Nanowires
ZnO
Sputtering

ABSTRACT

The structural and optical properties of SnO_2–ZnO core–shell nanowires were studied and the effects of thermal annealing were investigated. As-prepared SnO_2–ZnO core–shell nanowires exhibited a smooth and continuous shell layer along the nanowire, with a thickness in the range of 5–10 nm. While the thin ZnO shell layer disappeared after annealing at 800 °C, this did not occur after annealing at 600 °C. The as-fabricated SnO_2–ZnO core–shell nanowires exhibited yellow emission, presumably from the core SnO_2 nanowires. The UV emission from ZnO shell layer was obtained by annealing at 600 °C, whereas it was removed by annealing at 800 °C.

1. Introduction

Tin oxide (SnO_2) is a key functional material that has been used for optoelectronic devices, gas sensors, solar cells, and catalysts. In addition, zinc oxide (ZnO) is of great interest for electronic and photonic applications, including blue/UV photoelectronic devices [1,2]. Due to its extraordinary physical and chemical properties, other applications involving the use of ZnO include mechanics, field emission displays, spintronics, gas sensors, and biomedical sensors.

In recent years, core–shell nanowires have begun to attract interest as their functions can be further enhanced by fabricating the core and shell from different materials [3]. It is well known that the composite materials of ZnO and SnO_2 exhibit excellent physical and chemical properties that are superior to their individual materials [4]. For example, the photocatalytic activity was significantly enhanced in the case of a ZnO/SnO_2 composite catalyst in contrast with the catalytic activity of ZnO or SnO_2 powders [5]. In addition, ZnO/SnO_2 core–shell heterostructures exhibit unique luminescence properties [4]. The present study describes the synthesis and characterization of ZnO-coated SnO_2 nanowires. A simple and efficient two-step fabrication process is demonstrated in which the preparation of core SnO_2 nanowires is followed by the sputter-coating of ZnO shell layers. Furthermore, samples before and after thermal annealing are investigated for comparison.

2. Experimental

First, the core SnO_2 nanowires were synthesized by directly reacting Sn powders with O_2 in a horizontal furnace at 900 °C. A piece of Si wafer coated with Au film was used to gather the products. Subsequently, SnO_2 nanowires were coated using an RF sputter system in a manner described in the literature [6]. The sputtering was carried out using a ZnO target in a flow of Ar and O_2 gases. ZnO-coated SnO_2 nanowires were annealed in the range of 500–1000 °C. The product was investigated via X-ray diffraction (XRD) (Philips X'pert MRD diffractometer), scanning electron microscopy (SEM) (Hitachi, S-4200), and transmission electron microscopy (TEM) (Philips CM-200). The PL measurements were conducted under the excitation of a He–Cd laser (325 nm) in the UV region.

3. Results and discussion

Fig. 1a shows the XRD pattern of SnO_2–ZnO core–shell nanowires prior to thermal annealing. All of the diffraction peaks are

* Corresponding author. Tel.: +82 32 860 7544; fax: +82 32 862 5546.
E-mail address: hwkim@inha.ac.kr (H.W. Kim).

0925-3467/$ - see front matter © 2009 Elsevier B.V. All rights reserved.
doi:10.1016/j.optmat.2008.12.027

well indexed to the tetragonal rutile structure of SnO_2 (JCPDS file No. 41-1445). As ZnO-associated peaks are not clearly observed, it was assumed that the ZnO shell layer was sufficiently thin and/or amorphous. Fig. 1b shows the XRD pattern of SnO_2–ZnO core–shell nanowires annealed at 600 °C. Apart from the SnO_2-related peaks from the SnO_2 core, the appearance of new peaks associated with ZnO indicates the crystallization of amorphous ZnO shell layers. Fig. 1c shows the XRD pattern of SnO_2–ZnO core–shell nanowires annealed at 800 °C. Although reflection peaks from the core SnO_2 nanowires can be observed, ZnO-associated peaks cannot.

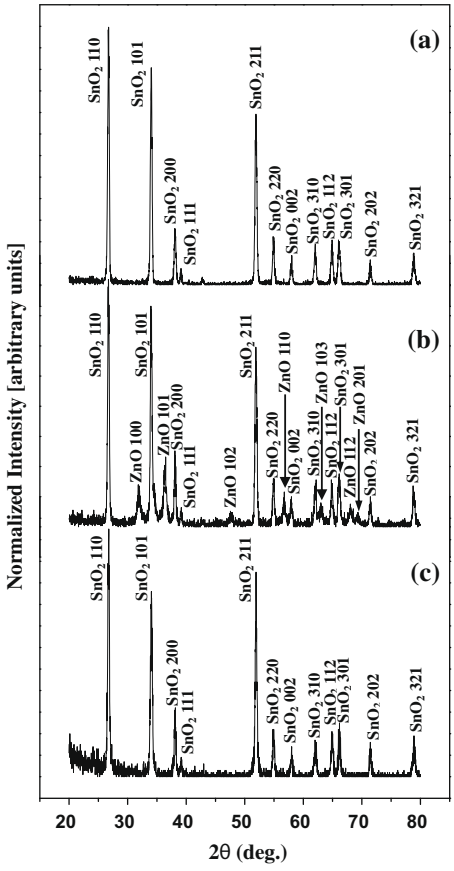

Fig. 1. XRD patterns of (a) as-fabricated SnO_2–ZnO core–shell nanowires, (b) SnO_2–ZnO core–shell nanowires annealed at 600 °C, and (c) SnO_2–ZnO core–shell nanowires annealed at 800 °C.

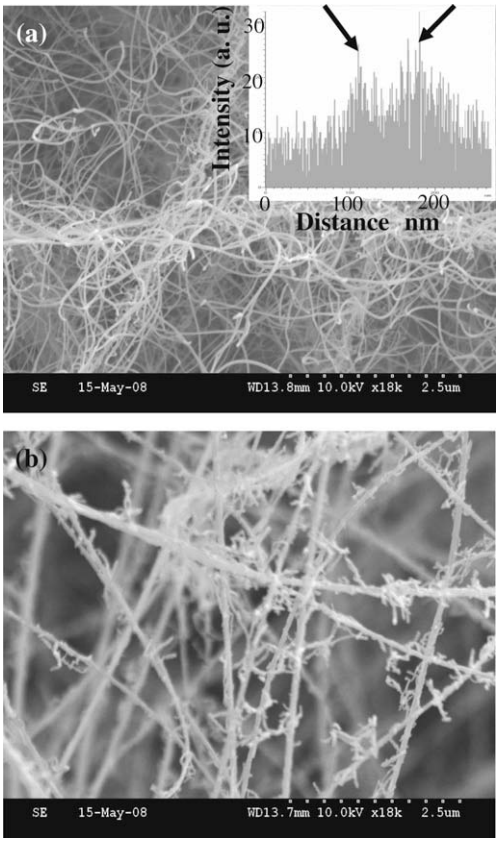

Fig. 3. (a) SEM image of SnO_2–ZnO core–shell nanowires annealed at 600 °C (Inset: corresponding TEM-EDX concentration profile of Zn, across the nanowire diameter). (b) SEM image of SnO_2–ZnO core–shell nanowires annealed at 800 °C.

Fig. 2a shows a low-magnification TEM image of as-fabricated SnO_2–ZnO core–shell nanowires. This figure clearly exhibits a rod-like core and thin coating layers (on both sides). The average thickness of the shell layer is approximately 5–10 nm. The typical lattice-resolved TEM image and its inset clearly result from a tetragonal rutile SnO_2 structure (Fig. 2b), indicating that the ZnO shell layer is thin and amorphous. Fig. 3a and b show SEM images of SnO_2–ZnO core–shell nanowires that were annealed at 600 °C and 800 °C, respectively. The inset of Fig. 3a shows the TEM-EDX

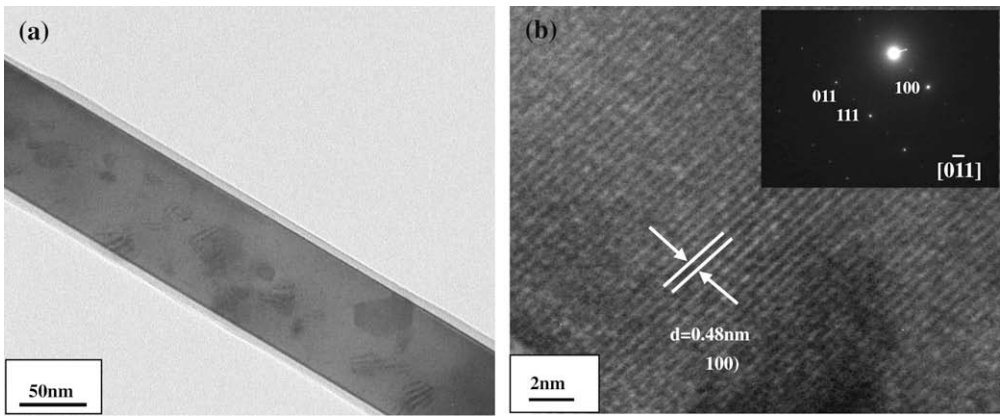

Fig. 2. (a) TEM image of an as-fabricated SnO_2–ZnO core–shell nanowire. (b) A typical lattice-resolved TEM image from (a), exhibiting the (1 0 0) lattice fringes of a tetragonal rutile SnO_2 (Inset: associated SAED pattern of the [0 $\bar{1}$ 1] zone axis of a tetragonal rutile SnO_2).

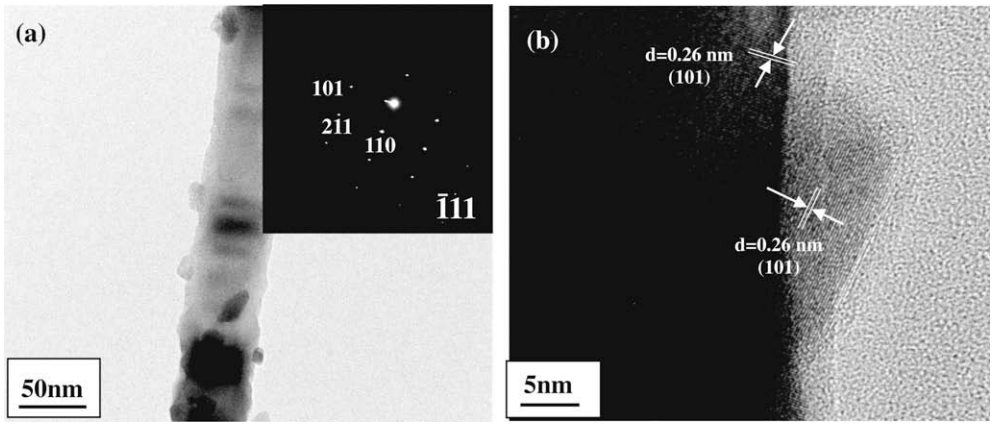

Fig. 4. (a) TEM image of a SnO_2–ZnO core–shell nanowires annealed at 800 °C (Inset: SAED pattern of the nanowire, which can be indexed as the $[\bar{1}\,1\,1]$ zone axis of a tetragonal rutile SnO_2). (b) Lattice-resolved TEM image enlarging an area near the surface of a 800 °C-annealed nanowire.

concentration profile of Zn across the diameter in a typical SnO_2–ZnO core–shell nanowire annealed at 600 °C. The highest peaks are in the sheath region (indicated by arrowheads), suggesting that Zn elements mainly reside in the shell region. Although the sample annealed at 600 °C exhibits a smooth 1D morphology, the sample annealed at 800 °C has a relatively rough surface. The TEM image indicates that the surface roughness of the sample annealed at 800 °C is attributable to the generation of cluster-like structures (Fig. 4a), presumably due to the effects of thermal heating. The inset of Fig. 4a shows an associated SAED pattern that can be indexed as the $[\bar{1}\,1\,1]$ zone axis of tetragonal rutile SnO_2. Fig. 4b is a lattice-resolved TEM image enlarging an area near the surface of the sample annealed at 800 °C. The interplanar spacing is approximately 0.26 nm, as it is indexed to the (1 0 0) plane of a tetragonal rutile SnO_2. The lattice-resolved image reveals that not only the central part but also the cluster-like structures of the sample annealed at 800 °C correspond to a tetragonal rutile SnO_2 phase. We surmise that the thermal heating induced the solid state diffusion and agglomoration of SnO_2 on the surface. Based on the XRD analysis, it was found that thermal annealing at 600 °C induced the transformation of an amorphous ZnO shell layer to the crystalline ZnO phase. On the other hand, after thermal annealing at a higher temperature of 800 °C, most of the ZnO phase disappeared. Although the associated mechanism is not clear at this point, it is well known that the decomposition of ZnO occurs at sufficiently high temperatures [7]. Solid ZnO can be sublimated to ZnO vapor, a part of which can decompose to Zn and O_2 vapor [7].

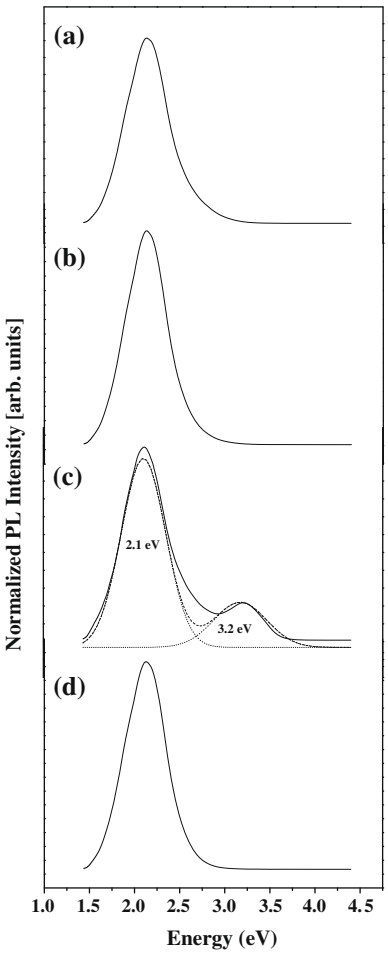

Fig. 5. Room temperature normalized PL spectra of (a) core SnO_2 nanowires, (b) as-fabricated SnO_2–ZnO core–shell nanowires, (c,d) SnO_2–ZnO core–shell nanowires annealed at (c) 600 °C and (d) 800 °C.

Fig. 5a shows the PL spectrum of the core SnO_2 nanowires measured at room temperature. It corresponds to a broad emission band that peaks at 2.1 eV around the yellow region. The yellow emission is ascribed to the trapped states within the bandgap, which was formed by the interaction of oxygen vacancies with interfacial tin or dangling bonds [8]. As shown in Fig. 5b, which shows the PL spectrum of the as-fabricated SnO_2–ZnO core–shell nanowires, the shape of the normalized PL spectrum was not altered by the ZnO coating. Fig. 5c is the PL spectrum of the SnO_2–ZnO core–shell nanowires annealed at 600 °C, indicating that the peak positions of two Gaussian bands are located at approximately 2.1 eV and 3.2 eV, respectively. While the emission band in the yellow region is assumed to originate from the SnO_2 core, the UV emission band around 3.2 eV can be associated with the excitons in ZnO [9,10]. It is assumed that the UV emission was very weak and not recognizable in the case of the as-fabricated SnO_2–ZnO core–shell nanowires. Although amorphous ZnO films can emit UV light [11], the ZnO shell layer in the present work will be sufficiently thin. On the other hand, after thermal annealing at 600 °C, the UV emission became strong enough to be observed in the spectrum. It is assumed that the ZnO shell layer became crystalline, apparently exhibiting UV light emission [12]. Fig. 5d shows the PL spectrum of SnO_2–ZnO core–shell nanowires annealed at 800 °C, revealing that the UV emission has disappeared. According to the XRD and TEM analyses, it is thought that the ZnO layer was removed due to high-temperature decomposition.

4. Conclusions

In summary, the coating of SnO_2 1D nanostructures with ZnO by means of RF sputtering is reported in this study. TEM imaging indicates that the ZnO shell layers in the range of 5–10 nm wrap the SnO_2 nanostructures after the sputter-coating process. The thin ZnO coating did not change the shape of the normalized PL spectrum significantly, whereas annealing at 600 °C caused additional UV emission. The UV emission was not found in the PL of samples annealed at 800 °C, presumably because the high-temperature annealing process removed the ZnO shell layers.

Acknowledgement

This work is the outcome of a Manpower Development Program for Energy & Resources supported by the Ministry of Knowledge and Economy (MKE) (No. 37112).

References

[1] W.D. Yu, X.M. Li, X.D. Gao, P.S. Qiu, W.X. Cheng, A.L. Ding, Appl. Phys. A 79 (2004) 453.
[2] R.F. Service, Science 276 (1997) 895.
[3] Y. Yin, Y. Lu, Y. Sun, Y. Xia, Nano Lett. 2 (2002) 427.
[4] Q. Kuang, Z.-Y. Jiang, Z.-X. Xie, S.-C. Lin, Z.-W. Lin, S.-Y. Xie, R.B. Huang, L.-S. Zheng, J. Am. Chem. Soc. 127 (2005) 11777.
[5] J. Bandara, K. Tennakone, P.P.B. Jayatilaka, Chemosphere 49 (2002) 439.
[6] H.W. Kim, N.H. Kim, Mater. Sci. Eng. B 103 (2003) 297.
[7] X.Y. Kong, Y. Ding, Z.L. Wang, J. Phys. Chem. B 108 (2004) 570.
[8] S.H. Luo, Q. Wan, W.L. Liu, M. Zhang, Z.T. Song, C.L. Lin, P.K. Chu, Prog. Solid State Chem. 33 (2005) 287.
[9] D.C. Reynolds, D.C. Look, B. Jogai, C.W. Litton, T.C. Collins, W. Harsch, G. Cantwell, Phys. Rev. B 57 (1998) 12151.
[10] S.W. Jung, W.I. Park, H.D. Cheong, G.-C. Yi, H.M. Jang, Appl. Phys. Lett. 80 (2002) 1924.
[11] Z. Wang, H. Zhang, Z. Wang, L. Zhang, J. Yuan, S. Yan, C. Wang, J. Mater. Res. 18 (2003) 151.
[12] Z.W. Zhao, B.K. Tay, J.S. Chen, J.F. Hu, X.W. Sun, S.T. Tan, Appl. Phys. Lett. 87 (2005) 251912.